Infrared look at the spectral effects of submicron confinements of CO$_2$ gas

J.-M. Hartmann,[1,*] X. Landsheere,[1] C. Boulet,[2] D. Sarkisyan,[3] A. S. Sarkisyan,[3] C. Leroy,[4] and E. Pangui[1]

[1]*Laboratoire Interuniversitaire des Systèmes Atmosphériques (LISA), CNRS (UMR 7583), Universités Paris-Est Créteil et Paris Diderot, and Institut P.-S. Laplace, Université Paris-Est Créteil, 94010 Créteil Cedex, France*

[2]*Institut des Sciences Moléculaires d'Orsay (ISMO), CNRS, Université Paris-Sud and Université Paris-Saclay, Orsay F-91405, France*

[3]*Institute for Physical Research, National Academy of Sciences of Armenia, Ashtarak, 0203 Armenia*

[4]*Laboratoire Interdisciplinaire Carnot de Bourgogne (ICB), CNRS (UMR 6303), Université Bourgogne Franche-Comté, 9 Avenue A. Savary, Boîte Postale 47 870, F-21078 Dijon Cedex, France*

We have recorded, near 4.3 μm, transmission spectra of pure CO$_2$ gas inserted between the windows of an extremely thin absorption cell. This was done for three pressures using a Fourier transform spectrometer and five optical paths between 0.17 and 1.15 μm. For these conditions, the line broadening induced by molecule-surface collisions can be studied under "clean" confinement conditions, i.e., between two parallel well-polished crystal surfaces separated by a known distance. This is in opposition with previous investigations using porous materials which involve pores of unknown dimensions with corrugated inner surfaces of ill-defined shapes. The analysis of the spectra shows that the line broadening due to the collisions of the molecules with the cell windows is independent of the optical transition and inversely proportional to the confinement length. Furthermore, the measured values are quantitatively reproduced if one assumes that a single CO$_2$-surface collision is sufficient to interrupt the rotating-dipole coherence. This gives a proof, here for the CO$_2$-sapphire system, of an assumption proposed many years ago and opens promising perspectives for the optical probing of porous materials.

While many studies have investigated the properties of tightly confined atomic vapors, including their absorption, fluorescence and magneto-optical spectra (e.g., [1-10] and those therein), much less has been done for molecules. The reason for this is likely that the intensities of their absorption lines being relatively small, tight confinements between parallel surfaces (thus very short optical paths) leads to very weak absorptions that are difficult to measure. All the available studies have hence used porous materials which provide significant paths [11,12] while confining the molecules in pores of submicron dimensions. Such investigations showed that the absorption lines are broadened (e.g., [12–15]) by the collisions of the molecules with the inner surfaces of the pores. However, the latter and the pore sizes and shapes are ill defined and unknown. Studying the absorption spectra of molecular gases under "clean" and controlled confinement conditions is thus relevant for two reasons. From the "fundamental" point of view it would bring information on molecule-surface collision processes. The variations of the resultant linewidths with the confinement length would enable a measurement of the efficiency of such collisions. Relating the confinement dimensions to the line broadening is also of "practical" interest since it would enable the optical probing of porous materials (e.g., aerogels, xerogels, ceramics) which have numerous important applications. Such porosimetry studies have been carried out [12,16,17], but they all relied on the not yet proven assumption that a single molecule-surface collision is sufficient to interrupt the radiation process. The main motivation of the present investigation is to check, under controlled confinement conditions, if this statement is true. The latter, suggested many years ago [18–22], leads to a simple relation between the line shapes and widths and the confinement characteristics, but it was not yet demonstrated experimentally.

For the experiments we used the thin cell shown in Fig. 1, similar to previous ones (e.g., [23]) used for studies of confined atomic vapors. It is composed of two well-polished crystalline sapphire windows (20 × 30 mm^2 and 2 mm thick) and of a connected tube in order to pump it out or fill it with gas. The windows are assembled in such a way that the distance between them varies from practically zero to a few microns, as indicated by the interference iridescence patterns in Fig. 1. More details on the cell design can be found in [23].

This cell was inserted into the (pumped-out) sample compartment of a Bruker IFS 120 Fourier transform spectrometer (FTS). It was localized at the focal point of the globar light where the beam diameter, governed by the 1.2-mm-wide iris used, is slightly greater than one millimeter (as visually checked using the visible light source of the spectrometer). The FTS was fitted with a globar source, a KBr beam splitter, and an InSb detector. The maximum optical path difference was set to 90 cm for a spectral resolution of 0.01 cm^{-1}, and about 1800 scans were coadded ($\simeq$20h of recording). The resulting noise on the transmissions (ratios of recordings made with CO$_2$ gas and an empty cell) is about $\pm 2 \times 10^{-4}$. Experiments were made at room temperature for pressures of about 0.1, 0.2, and 0.4 atm, measured with an MKS Baratron gauge (accuracy better than 0.3 mb in the investigated pressure range, checked by comparing the readings of three gauges). High-purity CO$_2$ gas was used. This species was retained because it is stable and has, among all molecules considered in the HIgh-resolution TRANsmission molecular absorption (HITRAN) database [24], the most intense lines in the transparency region of the cell windows. Five positions of the cell with respect to the light beam were used for a study of the influence of the optical path length (the confinement dimension) which varied between 0.17 and 1.15 μm. Note that the observed spectra are dominated by

---

*Corresponding author: hartmann@lisa.u-pec.fr

FIG. 1. The thin cell.

FIG. 2. Transmissions near the $P(16)$ line of the CO_2 ν_3 band at 0.19 atm for path lengths $L = 0.17$ and 0.41 μm (vertically shifted by -0.002). The symbols are measured values while the red lines are the calculated (fitted, see text) results.

the narrow lines of "free" CO_2 gas and do not show any broad structure attributable to adsorbed molecules, contrary to what was observed in a porous xerogel [12]. This is likely due to the fact that we here probe confinements involving much smaller surface-to-volume ratios, thanks to larger distances between the walls and the use of well-polished (and not corrugated) windows.

For the analysis of the spectra, the transmission at wave number σ, for a pressure P and a temperature T, was written as

$$\tau(\sigma,P,T) = \int_{-\infty}^{+\infty} F_{\text{inst}}(\sigma - \sigma')\exp[-\alpha(\sigma',P,T,L)L]d\sigma',$$
(1)

where F_{inst} is the FTS instrument function, L is the path length within the cell, and α is the absorption coefficient. The latter was computed by summing-up the contributions of all CO_2 optical transitions ℓ with Lorentz shapes i.e.,

$$\alpha(\sigma,P,T,L) = P \sum_{\text{lines } \ell} \frac{S_\ell(T)}{\pi} \frac{\Gamma_\ell^c(P,T,L)}{(\sigma - \sigma_\ell)^2 + \Gamma_\ell^c(P,T,L)^2}, \quad (2)$$

where σ_ℓ, S_ℓ, and Γ_ℓ^c are the position, integrated intensity, and collisional half width at half maximum (HWHM) of line ℓ, respectively. The measured transmissions were fitted using Eqs. (1) and (2) by floating L, σ_ℓ, and Γ_ℓ^c, while S_ℓ was fixed to the values provided by the HITRAN database [24]. With this approach, the path length and linewidths are thus determined from the same recording, ensuring that they correspond to the same localization in the cell (and thus the same thickness), a result difficult to achieve if L is determined independently (by interferometric means, for instance). Let us mention that the fitted values of σ_ℓ are, within uncertainties and their scatter from line to line, consistent with those given in [24]. In other words, no spectral shift is detected as was the case for CO_2 in a porous xerogel [12]. The fits were carried using microwindows around each retained line of CO_2. In each of them, a quadratic law ($a\sigma^2 + b\sigma + c$) multiplying the measured transmission was introduced in order to correct for biases in the measured
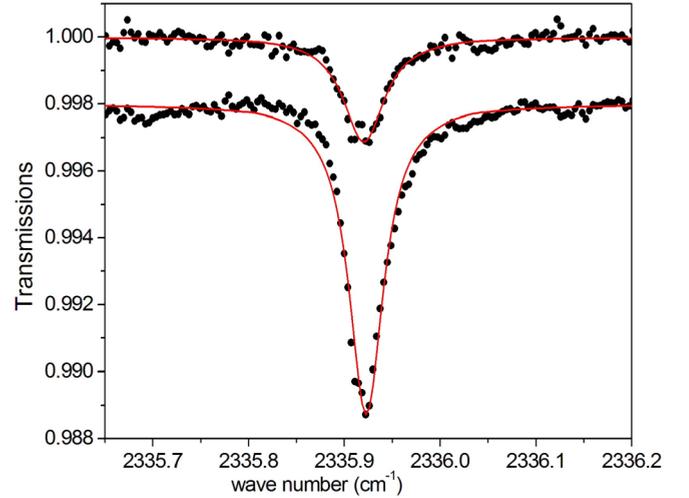
100% transmission level. Altogether, 35 lines [from $P(38)$ to $R(36)$ without the $P(2)$, $R(0)$, and $R(2)$] of the ν_3 band of $^{12}C^{16}O_2$ were retained because their absorptions are the largest. Examples of such fits, plotted in Fig. 2, show a good agreement between measured and calculated values. Despite the noise on the spectra and the absorption weakness (down to 0.2%), we thus expect reliable determinations of the optical path lengths and linewidths.

This is confirmed, in Fig. 3, by the values of L retrieved from the various CO_2 transitions ℓ, pressures P, and cell positions, since the results are almost independent of both ℓ and P. However, a detailed look at the values shows that there is, on average, a slight increase of L with P. The latter
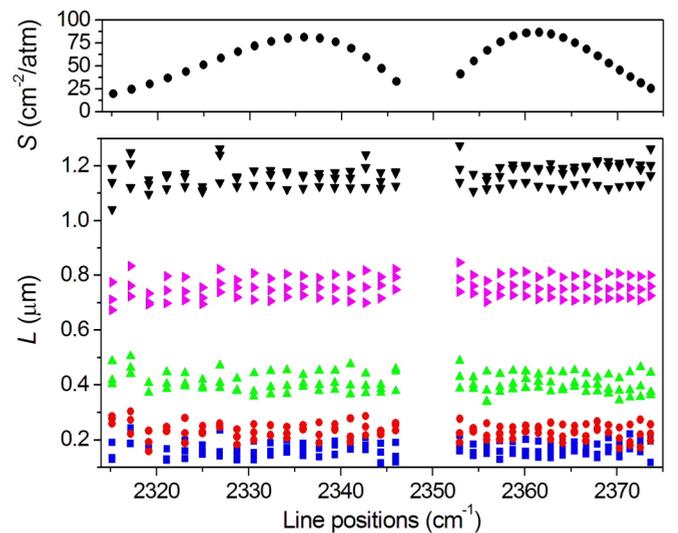

FIG. 3. The upper panel shows the line intensities S_ℓ from [24]. The lower panel displays the retrieved path lengths L for five positions of the cell with respect to the light beam as a function of the position σ_ℓ of the CO_2 line used (the three values for each σ_ℓ and cell position were obtained for the three pressures).
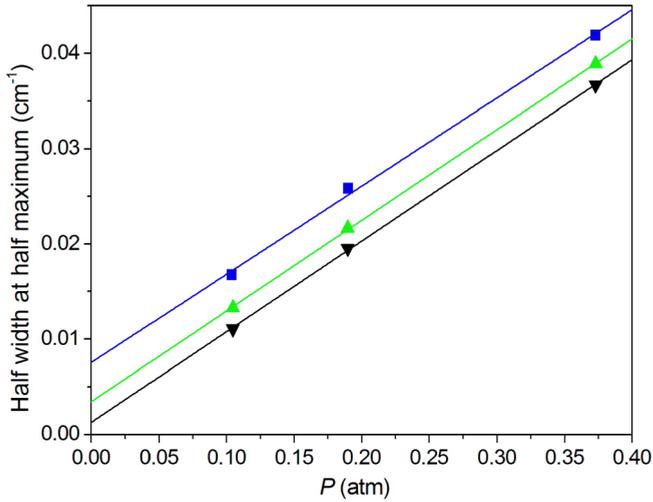
FIG. 4. Collisional half widths at half maximum (HWHMs) of the $P(16)$ line versus pressure. The symbols have been obtained for $L = 0.17$ (blue squares), 0.41 (green triangles), and 1.15 μm (black down triangles).

is probably due to the not full adequacy (see discussion after Fig. 6) of the Lorentzian line shape [Eq. (2)] used to fit the data. Nevertheless, this pressure dependence is moderate (typically 6% from the lowest to the highest pressure) and smaller than the scatter from line to line and thus does not significantly affect the determination of L. For the green triangles in Fig. 3, for instance, the averaged values of L over all lines are 0.395, 0.411, and 0.419 μm for $P = 0.10, 0.19,$ and 0.37 atm with standard deviations of about 0.03 μm. Averaging the 105 values for each cell position then leads to quite accurate determinations of the confinement size L (e.g., $\bar{L} = 0.408 \ \mu m$ with a standard deviation of 0.035 μm and a standard error of 0.003 μm for the green triangles in Fig. 3). Note that when all cell positions are considered, the standard deviation over all lines and pressures remains smaller than 15% of L.

As exemplified in Fig. 4 and observed previously [14,25], the linewidths Γ_ℓ^c vary linearly with P, with an extrapolated value at $P = 0$ that depends on L (while the slope practically does not). They were thus fitted using the linear law

$$\Gamma_\ell^c(P,T,L) = \Gamma_\ell^W(T,L) + P\gamma_\ell(T), \quad (3)$$

in which the second term results from interactions between CO_2 molecules while the first one represents the effects of collisions of the molecules on the cell windows.

Considering first the fitted values of $\gamma_\ell(T)$, they are, despite the noise on the spectra, in good agreement with the "usual" collisional linewidths (for unconfined gas) as given in the HITRAN data base [24] and measured in [26]. For instance, the slopes of the three linear fits in Fig. 4 are only 5% different from the free gas pressure broadening coefficient given in [26]. As for $\Gamma_\ell^W(T,L)$, the results show that they are, within experimental errors, independent of the transition, as observed for several gases inside a porous silica xerogel [12]. The values of $\Gamma_\ell^W(T,L)$ obtained from the 35 CO_2 lines ℓ have thus been averaged, leading to a final set of five determinations of $\Gamma^W(T,L)$ for L between 0.17 and 1.15 μm. For the uncertainties (error bars) we retained twice the standard

error on the averaged values of Γ^W and L for $\Delta\Gamma^W$ and ΔL. The latter was further increased by 8% of L, in order to include the dispersion due to the above mentioned pressure dependence and to take into account the uncertainties on the line intensities S_ℓ used [24] in the fits of the spectra. The (very) small errors affecting the pressure and temperature measurements have been neglected.

In order to theoretically predict $\Gamma^W(T,L)$, a simple model can be developed, generalizing the developments made in [12,15]. As shown in the Appendix, for a one-dimensional confinement of length L, and for our specific experimental conditions, the dipole autocorrelation function (ACF) for a single absorption line can be written as

$$\Phi(t,P,T) = \exp(-\gamma Pt)\left(\text{erf}\left[\sqrt{\frac{m}{2k_BT}} \frac{L}{t} \right] \right.$$
$$\left. - \frac{t}{L}\sqrt{\frac{2k_BT}{\pi m}}\left[1 - \exp\left(-\frac{m}{2k_BT}\frac{L^2}{t^2} \right) \right] \right), \quad (4)$$

in which m is the molecular mass, k_B the Boltzmann constant, and erf($\cdot$) the error function. The first exponential term takes into account the effects of CO_2-CO_2 interactions through the free-gas broadening coefficient per unit pressure γ. Using Eq. (4), one can compute the area-normalized line shape from

$$\alpha(\Delta\omega,P,T) = \pi^{-1}\text{Re}\left[\int_0^\infty \exp(-i\Delta\omega t)\Phi(t,P,T)dt \right]. \quad (5)$$

The spectra predicted for various pressures can then be treated as was done for the experimental ones in order to retrieve the HWHM due to molecule-surface collisions. Things can be even simpler if one approximates the ACF of Eq. (4) by an exponential decay having the same slope at $t = 0$. One then obtains

$$\Phi^{app}(t,P,T) = \exp\left\{ -\left[\frac{1}{L}\sqrt{\frac{2k_BT}{\pi m}} + P\gamma \right]t \right\}, \quad (6)$$

which leads, through Eq. (5), to a Lorentzian line shape in which the contribution of molecule-wall collisions to the broadening is (here expressed in s^{-1}, which can be converted to cm^{-1} by dividing by $2\pi c$)

$$\Gamma^W(T,L) = \frac{1}{L}\sqrt{\frac{2k_BT}{\pi m}} = \frac{\bar{v}_\perp(T)}{L}, \quad (7)$$

where $\bar{v}_\perp(T)$ is the mean molecular speed along the axis perpendicular to the cell windows. This result expresses the fact that, within the assumed model, $1/\Gamma^W$ is simply the average time between successive molecule-window collisions. Equations (4) and (5), and the much easier to use Eq. (7), which can be generalized to two- and three-dimensional situations [12,22], have the great interest, for optical probings, of approximately but directly relating the broadening to the confinement dimension.

The results of the two theoretical approaches are compared with the measured values of Γ^W in Fig. 5, showing a satisfactory agreement. For a comparison based on numbers, we have adjusted these values by the law $\Gamma^W(L) = A/L$ in which A is the fitted parameter, unitless if L is expressed in cm. Note that, consistently with Eq. (7), A can be converted to speed units (cm/s) by multiplying it by $2\pi c$. The fit of the
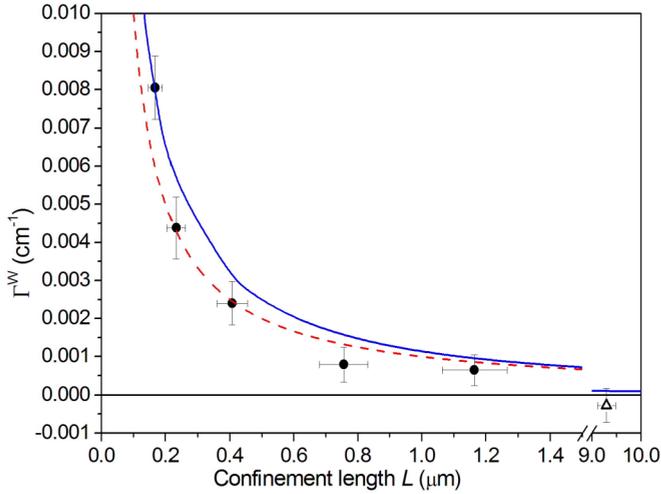
FIG. 5. Line widths (HWHMs) due to collisions of the CO_2 molecules with the cell windows as a function of the confinement length. The full circles are experimentally determined values from the present study while the open triangle was obtained from the measurements of [26]. The red dashed line gives predictions of Eq. (7) while the blue line was obtained from spectra computed using Eqs. (4) and (5) for the three measured pressures and treated as the experimental ones.

FIG. 6. (a) Dipole ACFs computed from Eq. (4) for CO_2 at 296 K, $L = 0.2 \ \mu m$, and $\gamma P = 0$ (black circles). The dashed blue line is the exponential decay giving the associated best fit and the full red line shows the results of Eq. (6). (b) Line shapes computed from Eqs. (4) and (5) (symbols) and corresponding Lorentzian fits (lines) for CO_2 at 296 K, $L = 0.2 \ \mu m$,, $\gamma = 0.1 \ cm^{-1}$/atm, and $P = 0.02$ atm (black circles and full red line) and 0.1 atm (blue triangles and dashed black line).

experimental values leads to $A = (1.2 \pm 0.15) \times 10^{-7}$. while that of the theoretical profile [Eqs. (4) and (5); blue line] leads to $A = (1.28 \pm 0.06) \times 10^{-7}$ (error bars being twice the standard deviation). Finally the simple model of Eqs. (4), (6), and (7) gives $A = 1.0 \times 10^{-7}$. The consistency between these numbers (and particularly the first two) validates the proposed model and thus the assumption of the full efficiency of molecule-wall collisions. As for the difference (around 25%) between the A values deduced from the two models, it is a consequence of the nonexponential behavior of the correlation function in Eq. (4) as further discussed below.

Note that, up to now, we have neglected the influence of the finite size of the infrared beam. In fact, the cell thickness varying across the beam, the resulting absorption is an average of line profiles associated with various optical paths and having different linewidths due to different confinements. From the five localizations of the beam in the cell and the associated retrieved lengths L, the variation of the path length over the beam radius (0.6 mm) is estimated to be of 25% at the most. Numerical simulations using Lorentz line shapes, Eq. (7), and L varying between $0.75\bar{L}$ and $1.25\bar{L}$, have then been carried out. They show that the absorption averaged over the beam size is practically identical to that calculated for the mean length $\bar{L}$. The influence of the averaging on the line area and line width being smaller than 1% (in the worst case of $\bar{L} = 0.15 \ \mu m$), the influence of the finite size of the beam can indeed be safely neglected.

Coming back to the differences between the two theoretical curves in Fig. 5, they can be explained by the time dependences of the dipole ACFs in Eqs. (4) and (6). Indeed, Fig. 6(a) shows that they deviate from each other, Eq. (6) underestimating the decay at short times although it has the proper slope at $t = 0$. This underestimation results, in the
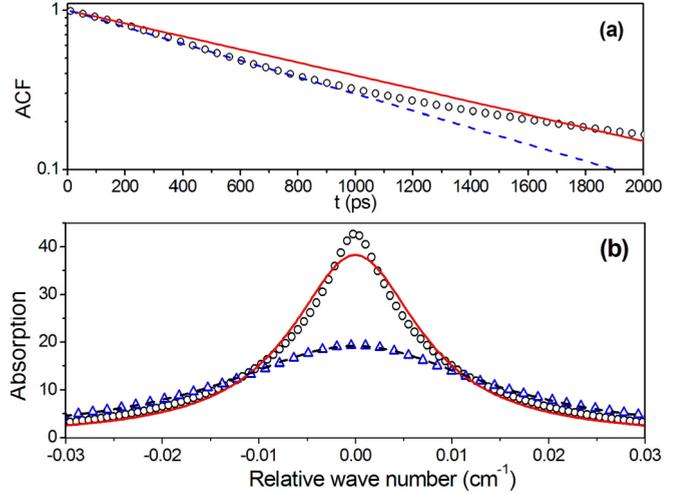
spectral domain, in a smaller value of $\Gamma^W(L)$ as can be seen in Fig. 5. If we now consider the line shape, Fig. 6(b) shows that deviations from the best-fitted Lorentzian profile are important when the broadening due to molecule-surface collisions is non-negligible when compared to that $(P\gamma)$ resulting from molecule-molecule interactions. This can be explained by looking at the prediction of Eq. (4) (circles) and the best exponential decay fit (dashed blue curve) in Fig. 6(a). Indeed, for large enough pressures, the decay induced by the $\exp(-\gamma Pt)$ in Eq. (4) cuts off the region $(t > 1000 \text{ ps})$ where the ACF deviates from a pure exponential so that the resulting profile is practically Lorentzian. On the opposite side, at low pressures, the long-time behavior does play a role. Since the ACF there decreases more slowly than its best fit by an exponential decay, the resulting profile is narrower than a Lorentzian with deviations reaching 10% of the peak absorption for 0.02 atm (while they are smaller than 1% for 0.1 atm).

While we believe that the present study has proven that, for thermal CO_2 gas and a sapphire window, a single molecule-surface collision interrupts the radiation process, the question of how this happens remains open, i.e., is it due to adsorption, to a strong dephasing of the rotating dipole, or to a change in the rotational quantum number J?. Considering adsorption, we think it does not play a significant role because the spectra do not show any signature (seen in [12] for instance) of adsorbed molecules. In other words (most) molecules quickly bounce on the surface. As for the dephasing process, it should be very efficient in order to scramble the phase enough to destroy the coherence of the rotating dipole. If one considers intermolecular collisions, this dephasing leads, in the spectral domain, to a shifting of the absorption lines. Nevertheless, it is well known that for most molecular systems this shift is

much smaller than the line broadening (about two orders of magnitude for CO_2 in the ν_3 band [24]), the latter mainly resulting from collision-induced changes of the rotational speed. We thus believe that for molecule-surface collisions this is also the case and that the broadening observed in this paper is due to the fact the interaction of a molecule with the surface efficiently changes to rotational quantum number J. This is consistent with what was derived from a previous analysis of gases confined in a xerogel sample [27]. Another issue is the generality of the full efficiency of molecule-surface collisions to interrupt the radiation process. At this stage, our guess is that it is valid for many other systems, except probably for very "soft" surfaces (with which molecules interact through a weak and slowly varying anisotropic interaction potential) or very high rotational states (i.e., "super-rotors" [28] spinning so quickly that they become almost insensitive to the anisotropy of the molecule-surface interaction). In connection with these issues, an extension of the present work would be to study the influences of the molecular mass and of the temperature in order to further assess the validity of Eqs. (4) and (7). In addition, studying the deviations of the observed line shapes from the Lorentzian profile would obviously provide more detailed information on molecule-wall collisions. However, while the signal-to-noise ratio of the FTS spectra enabled sufficiently accurate determinations of the path length and line-broadening using the extremely intense lines of the CO_2 ν_3 band, it is too limited for such studies. Indeed, other molecular species (e.g., CH_4, H_2O, CO, OCS) with different masses have significantly smaller [24] line intensities than CO_2 which make their absorptions too small for reliable analyses with a FTS. Similarly, the non-Lorentzian effects are expected [Fig. 6(b)] to be in practise within the noise of FTS spectra. A way to overcome these limitations, currently under investigation, may be to use tunable lasers which emit radiation in the relevant 3–5 μm region. Note that the crystalline sapphire of the cell windows is transparent in the 0.16–6.5 μm range, and is thus adapted for such studies.

APPENDIX: CALCULATION OF THE DIPOLE CORRELATION IN A ONE-DIMENSIONAL CONFINED MOLECULAR GAS

We here present a semiclassical treatment that leads, in the proper limit, to the expression of the dipole correlation function as given by Eq. (4). This treatment generalizes early calculations [19–22] by taking into account both molecule-molecule and molecule-wall collisions. Meanwhile, it will be shown that the present model is strictly equivalent to that developed in [29] in the frequency domain, instead of working in the time-domain as in [15].

We consider a molecular gas confined between two infinite parallel planar walls located at $x = \pm L/2$ and look at the spectrum at angular frequencies ω close to an isolated transition centered at ω_0. Classically, a radiative dipole will emit, in the direction $+x$ of the detector, a plane wave, damped

by the effects of molecule-molecule collisions, and given by

$$\exp[-\gamma(v_x)Pt]\exp[i(\omega - \omega_0 - kv_x)t], \quad \text{(A1)}$$

where v_x is the radiator velocity component along the wave propagation direction, $k = 2\pi/\lambda$ is the amplitude of the wave vector, and kv_x is the Doppler shift. $\gamma(v_x)P$ is the velocity-dependent collisional width due to molecule-molecule interactions at the considered pressure P. In the following we neglect the small (e.g., [30]) velocity dependence of the linewidth so that $\gamma(v_x)$ becomes the "usual" collisional broadening coefficient γ. We also assume that the interactions between the molecules do not, on average, change the value of v_x and that any collision with the windows of the cell interrupts the radiative process. We must then distinguish two classes of velocity, namely, $v_x > 0$ and $v_x < 0$.

Starting from Eq. (A1), the emitted field due to all the molecules moving in the $+x$ direction is proportional to:

$$\int_0^{+\infty} dv_x f_{MB}(v_x)\frac{1}{L}\int_{-L/2}^{+L/2} dx \int_0^{(L/2-x)/v_x} dt e^{-\Lambda t}, \quad \text{(A2)}$$

where x is the position of a molecule at $t = 0$, $f_{MB}(v_x)$ is the Bolzmann distribution for the v_x velocity component, and we introduced the complex quantity $\Lambda = \gamma P - i(\omega - \omega_0 - kv_x)$. Similarly, the contribution of the molecules moving in the opposite direction is given by

$$\int_{-\infty}^{0} dv_x f_{MB}(v_x)\frac{1}{L}\int_{-L/2}^{+L/2} dx \int_0^{(L/2+x)/v_x} dt e^{-\Lambda t}. \quad \text{(A3)}$$

At that step, and in order to go further, two paths can be followed: In the first one, the integrals over x and t are explicitly calculated, leading, from the sum of the positive and negative velocity contributions, to the following line profile:

$$\int_{-\infty}^{+\infty} dv_x f_{MB}(v_x)\frac{1}{\Lambda}\left\{1 - \frac{|v_x|}{\Lambda L}[1 - \exp(-\Lambda L/|v_x|)]\right\}. \quad \text{(A4)}$$

It should be emphasized that Eq. (A4) is exactly that derived from Bloch equations in [29], for instance. It was then used later on for studies on confined atomic vapors (e.g., [9,10]).

Here, rather than working in the frequency domain, we prefer to first change the integration ranges in Eq. (A2) from

$$v_x \in [0, +\infty], \quad t \in [0,(L/2 - x)/v_x]$$

to

$$t \in [0, +\infty], \quad v_x \in [0,(L/2 - x)/t],$$

with quite similar changes in (A3). We then obtain the following expression of the line shape:

$$\int_0^{+\infty} dt e^{i(\omega-\omega_0)t} e^{-\gamma Pt}\frac{1}{L}\int_{-L/2}^{+L/2} dx$$
$$\times \int_{-(L/2+x)/t}^{(L/2-x)/t} dv_x f_{MB}(v_x)e^{-ikv_x t}, \quad \text{(A5)}$$

which can be also written, using parity considerations, as

$$\int_0^{+\infty} dt e^{i(\omega-\omega_0)t} e^{-\gamma Pt}\frac{1}{L}\int_{-L/2}^{+L/2} dx$$
$$\times \int_{-(L/2+x)/t}^{(L/2-x)/t} dv_x f_{MB}(v_x)\cos(kv_x t). \quad \text{(A6)}$$

Important orders of magnitude. First of all, let us note that our experimental conditions are not at all those of [9,10]. In these studies, the cell length L was of the order of (or higher than) the wavelength λ and the width γP was much smaller than the Doppler broadening, allowing the observation of sub-Doppler features. In our conditions, L is much smaller than λ, and γP is from about 5 to 15 times larger than the Doppler width. It is thus not surprising that such very different conditions lead to very different experimental features. Here, in the integral over v_x in Eq. (A6), $v_x t$ is, at worst, of the order of L, and since $L \ll \lambda$ one can approximate $\cos(k v_x t)$ by 1. In other words, there is a complete Dicke effect which completely cancels the role of the Doppler shifts and of the resulting transient effects. We will not develop here the end of the calculation leading to Eq. (4), since it can be found in [15] where the Doppler contribution was *a-priori* omitted.

[1] D. Sarkisyan, D. Bloch, A. Papoyan, and M. Ducloy, Opt. Commun. **200**, 201 (2001).

[2] G. Dutier, A. Yarovitski, S. Saltiel, A. Papoyan, D. Sarkisyan, D. Bloch, and M. Ducloy, Europhys. Lett. **63**, 35 (2003).

[3] M. Fichet, G. Dutier, A. Yarovitsky, P. Todorov, I. Hamdi, I. Maurin, S. Saltiel, D. Sarkisyan, M.-P. Gorza, D. Bloch, and M. Ducloy, Europhys. Lett. **77**, 54001 (2007).

[4] A. Sargsyan, G. Hakhumyan, C. Leroy, Y. Pashayan- Leroy, A. Papoyan, and D. Sarkisyan, Opt. Lett. **37**, 1379 (2012).

[5] J. Keaveney, A. Sargsyan, U. Krohn, I. G. Hughes, D. Sarkisyan, and C. S. Adams, Phys. Rev. Lett. **108**, 173601 (2012).

[6] J. Keaveney, I. G. Hughes, A. Sargsyan, D. Sarkisyan, and C. S. Adams, Phys. Rev. Lett. **109**, 233001 (2012).

[7] K. A. Whittaker, J. Keaveney, I. G. Hughes, A. Sargsyan, D. Sarkisyan, and C. S. Adams, Phys. Rev. Lett. **112**, 253201 (2014).

[8] A. Sargsyan, A. Tonoyan, G. Hakhumyan, C. Leroy, Y. Pashayan-Leroy, and D. Sarkisyan, Europhys. Lett. **110**, 23001 (2015).

[9] S. Briaudeau, S. Saltiel, G. Nienhuis, D. Bloch, and M. Ducloy, Phys. Rev. A **57**, R3169 (1998).

[10] G. Dutier, S. Saltiel, D. Bloch, and M. Ducloy, J. Opt. Soc. Am. B **20**, 793 (2003).

[11] T. Svensson, E. Adolfsson, M. R. Lewander, C. T. Xu, and S. Svanberg, Phys. Rev. Lett. **107**, 143901 (2011).

[12] J. Vander Auwera, N. H. Ngo, H. El Hamzaoui, B. Capoen, M. Bouazaoui, P. Ausset, C. Boulet, and J.- M. Hartmann, Phys. Rev. A **88**, 042506 (2013).

[13] Y. N. Ponomarev, T. M. Petrova, A .M. Solodov, and A. A. Solodov, Opt. Express **18**, 26062 (2010).

[14] C. T. Xu, M. Lewander, S. Andersson-Engels, E. Adolfsson, T. Svensson, and S. Svanberg, Phys. Rev. A **84**, 042705 (2011).

[15] J.-M. Hartmann, V. Sironneau, C. Boulet, T. Svensson, J. T. Hodges, and C. T. Xu, Phys. Rev. A **87**, 032510 (2013).

[16] T. Svensson, E. Adolfsson, M. Burresi, R. Savo, C. T. Xu, D. S. Wiersma, and S. Svanberg, Appl. Phys. B: Lasers Opt. **110**, 147 (2013).

[17] T. M. Petrova, Y. N. Ponomarev, A. A. Solodov, A. M. Solodov, and A. F. Danilyuk, JETP Lett. **101**, 65 (2015).

[18] R. H. Johnson and M. W. P. Strandberg, Phys. Rev. **86**, 811 (1952).

[19] M. Danos and S. Geschwind, Phys. Rev. **91**, 1159 (1953).

[20] S. C. M. Luijendijk, J. Phys. B: At. Mol. Phys. **18**, 2995 (1975).

[21] S. L. Coy, J. Chem. Phys. **73**, 5531 (1980).

[22] P. E. Wagner, R. M. Somers, and J. L. Jenkins, J. Phys. B: At. Mol. Opt. Phys. **14**, 4763 (1981).

[23] A. Sargsyan, G. Hakhumyan, R. Mirzoyan, and D. Sarkiyan, JETP Lett. **98**, 441 (2013).

[24] L. S. Rothman, I. E. Gordon, Y. Babikov, A. Barbe, D. C. Benner, P. F. Bernath, M. Birk, L. Bizzocchi, V. Boudon, L. R. Brown, A. Campargue *et al.*, J. Quantum Spectrosc. Radiat. Transfer **130**, 4 (2013).

[25] J.-M. Hartmann, C. Boulet, J. Vander Auwera, H. El Hamzaoui, B. Capoen, and M. Bouazaoui, J. Chem. Phys. **140**, 064302 (2014).

[26] N. H. Ngo, X. Landsheere, E. Pangui, S. Morales, and J.-M. Hartmann, J. Mol. Spectrosc. **306**, 33 (2014).

[27] H. Tran, J. Vander Auwera, X. Landsheere, N. H. Ngo, E. Pangui, S. B. Morales, H. El Hamzaoui, B. Capoen, M. Bouazaoui, C. Boulet, and J.-M. Hartmann, Phys. Rev. A **92**, 012707 (2015).

[28] Y. Khodorkovsky, U. Steinitz, J.-M. Hartmann, and I. S. Averbukh, Nat. Commun. **6**, 7791 (2015).

[29] B. Zambon and G. Nienhuis, Opt. Commun. **143**, 308 (1997).

[30] V. Malathy Devi, D. C. Benner, L. R. Brown, C. E. Miller, and R. A. Toth, J. Mol. Spectrosc. **242**, 90 (2007).